Inorganic Chemistry

ARTICLE

pubs.acs.org/IC

Examination of the Silver Colloid Binding Behavior of Disulfide-Tethered Bipyridine Ligands and Their *fac*-Tricarbonylrhenium(I) Complexes

Heather J. Montgomery, Diane Pelleteret, Steven E. J. Bell, and Nicholas C. Fletcher*

School of Chemistry and Chemical Engineering, Queen's University of Belfast, David Keir Building, Belfast, Northern Ireland, U.K. BT9 5AG

Supporting Information

ABSTRACT: The syntheses of 2,2′-bipyridin-5-ylmethyl-5-(1,2-dithiolan-3-yl)pentanoate (**L1**) and *N*-(2,2′-bipyridin-5-ylmethyl)-5-(1,2-dithiolan-3-yl)pentanamide (**L2**) and their neutral *fac* carbonylrhenium(I) complexes [Re(**L1**)$(CO)_3$Br] and [Re(**L2**)$(CO)_3$Br] are reported. The electronic absorption and emission spectra of the complexes are similar to the spectrum of the reference compound [Re(bipy)$(CO)_3$Br] and correlate well with the density functional theory calculations undertaken. The surface-enhanced Raman spectroscopy (SERS) spectra (excited at both 532 and 785 nm) of the ligands and complexes were examined and compared to the spectrum of ethyl 5-(1,2-dithiolan-3-yl)pentanoate (**L3**), revealing that there is very little contribution to the spectra of these species from the dithiolated alkyl chains. The spectra are dominated by the characteristic peaks of a metalated 2,2′-bipyridyl group, arising from the silver colloid/ion complexation, and the rhenium center. The rhenium complexes show weak SERS bands related to the CO stretches and a broad band at 510 cm^{-1} assigned to Re−CO stretching. Concentration-dependent studies, measured by the relative intensity of several assigned peaks, indicate that, as the surface coverage increases, the bipyridine moiety lifts off the surface. In the case of **L1** and **L2**, this gives rise to complexes with silver at low concentration, enhancing the signals observed, while for the tricarbonylbromorhenium complexes of these ligands, the presence of the disulfide tether allows an enhancement in the limits of detection of these surface-borne species of 20 times in the case of [Re**L2**$(CO)_3$Br] over [Re(bipy)$(CO)_3$Br].

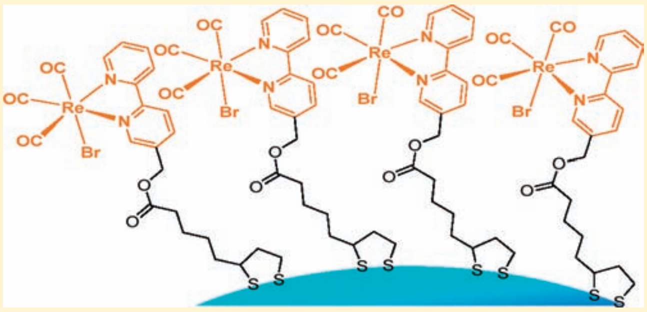

■ INTRODUCTION

Recent years have seen a growing interest in the long-lived excited states of the tricarbonyldiimine complexes of rhenium(I).[1] In contrast to the widely studied polypyridyl complexes of ruthenium,[2] controlling the inherent geometrical isomerism in the *fac*-tricarbonylrhenium(I) moiety is synthetically much less demanding, having just three available coordination sites, two of which are occupied with the chelating bipyridine, which gives rise to the characteristic metal-to-ligand charge-transfer (MLCT) luminescence. The final site is occupied by a spectator ligand. Such species have already been shown to have application in a diverse range of materials designed for charge transfer,[3] photocatalytic reduction of carbon dioxide,[4,5] molecular recognition,[6,7] biological sensing,[7,8] and cell imaging.[3,9] However, to develop these properties into working devices, it is necessary to tether these complexes to a support. Gold and silver surfaces have been widely considered in this respect, possessing a high affinity for alkanethiols.[10] Surprisingly though, the number of reports of 2,2′-bipyridine (bipy) groups bearing a thiolated group remains small,[11,12] and of these, there is only a single recent report of a complex functionalized to a *fac*-carbonylrhenium(I) moiety.[12]

The introduction of self-assembled monolayers (SAMs) of thiolated modifiers on nanostructured gold and silver surfaces has recently led to considerable advances in chemical sensing and optical imaging applications.[13] With such systems, surface-enhanced Raman (SERS) and resonance Raman (SERRS) spectroscopies provide an extremely sensitive detection technique. Typically, the surface is modified with compounds that increase the binding affinity of the target species, and the Raman signature of the adsorbed target is recorded directly. This approach has been successfully applied to targets as diverse as blood glucose[14] and polycyclic aromatic hydrocarbons.[15] An alternative methodology is to use modifiers, which are more selective; in such systems, the Raman signal of the target may not be read directly, but the binding event is signaled by a change in the spectrum of the modifier. This approach is less commonly applied but has been demonstrated for metal binding ligands and surface-bound antibodies, which change the conformation on target conjugation.[16]

Received: May 10, 2010
Published: March 10, 2011

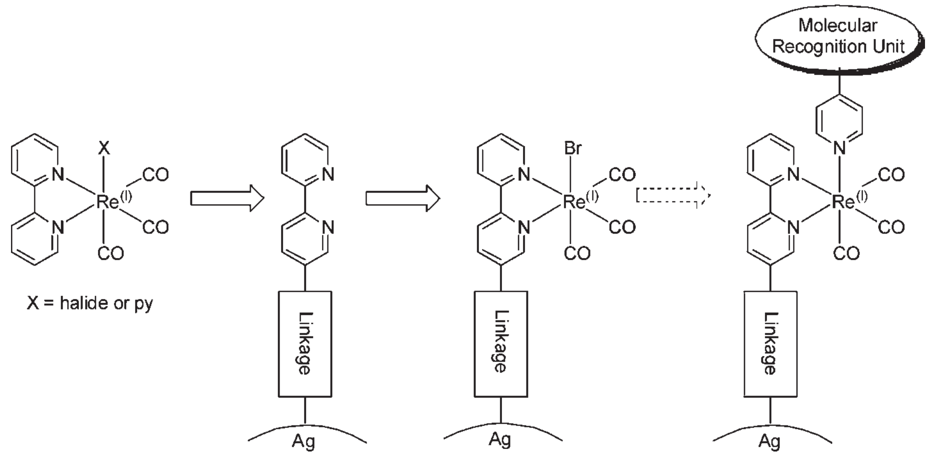

Figure 1. Schematic illustration of the design of a sensing platform, free chromophore, surface-bound chelation group, and surface-bound rhenium chromophore and the future design of a molecular sensing group.

There are remarkably few studies that have demonstrated isolation of the *fac*-carbonyldiiminerhenium(I) complexes on silver or gold surfaces; Vlčková and co-workers showed that $[Re(CO)_3LBr]$ [where L is either 2,3-bis(2′-pyridyl)pyrazine (dpp) or 2,2′-bipyrimidine (bpm)] could be detected by SERS using ligands to bridge between the metal and colloid surface but were unable to detect $[Re(CO)_3(bipy)Br]$,[17] while Ehler et al. demonstrated that using a thiolated pyridyl tether coordinated to rhenium resulted in SAMs that could be detected by both surface plasmon resonance and SERS.[18] Adopting a similar approach, Hallett et al. have recently reported a complex tethered to gold nanoparticles through a thioester-terminated alkyl chain attached via a nicotinamide group to the sixth site of a *fac*-carbonyldiiminerhenium(I) center.[19] In this particular case, the emissive behavior was investigated, indicating that the wavelength and lifetime of the complex itself surprisingly are not affected by the presence of the gold nanoparticles, despite the known ability of the particles to quench long-lived excited states.

In recent years, we have been exploring the possibility of developing sensing technologies from tricarbonyldiimine complexes of rhenium(I), having recently reported a dinuclear complex with selective enhancement of luminescence in the presence of dihydrogenphosphate.[20] In an extension to this study, a modular approach was developed to create bimetallic complexes, bearing both ruthenium(II)- and rhenium(I)-based lumophores.[21] In this paper, we discuss isolation of a new range of bipyridine complexes bearing an appropriate dithiol functionality to tether the complexes to silver nanoparticles and the subsequent investigation of the behavior of both the ligand itself and rhenium(I) on an aggregated silver colloid surface probed by SERS. This forms the initial investigation within a larger research program (Figure 1), exploring the preparation of rhenium-modified surfaces to be used as a platform on which we can append appropriate substituents to probe biological activity, at a molecular level. By exchange of the halide for a phosphane or pyridyl in situ, it is possible to use a well-defined and understood transition-metal coordination methodology over the more complex chemistry usually associated with the modification and isolation of SAMs on colloidal nanoparticles. Further, the rhenium(I) chromophore acts not only as an appropriate structural scaffold but also as a transducer of a “sensed” event, through a change in either the emissive behavior or enhanced resonance Raman spectroscopy, thereby amplifying signals arising from both the lumophore and the nanoparticles themselves.

■ EXPERIMENTAL SECTION

Instrumentation. ^1H and ^{13}C NMR spectra were recorded on Bruker DPX 300 and DRX 500 spectometers using the solvent as an internal reference, electronic spectra were recorded on a Perkin-Elmer Lambda 800 spectrophotometer, emission spectra were recorded on a Perkin-Elmer LS55 spectrofluorimeter in aerated CH_3CN at 298 K with the sample concentration adjusted to give an absorption of 0.1 in a 1 cm cell at an excitation wavelength of 400 nm, and emission quantum yields (Φ_{em}) were calculated relative to $[Re(CO)_3Br(bipy)]$ (7.8×10^{-3})[22] in acetonitrile. IR spectra were recorded as KBr disks on a Perkin-Elmer Spectrum RX I Fourier transform infrared system. Raman spectra were recorded on an Avalon Instruments/Perkin-Elmer RamanStation with an excitation wavelength of 785 nm and a RamanStation R3 with an excitation wavelength of 532 nm coupled to an Olympus CX21 microscope via a fiber-optic cable. Microanalyses and electron impact/electrospray (EI/ES) mass spectrometry was performed by “ASEP”, School of Chemistry and Chemical Engineering, Queen’s University Belfast.

Materials. All starting materials were used as received from the supplier. Laboratory-grade solvents were used unless otherwise specified. Dichloromethane (DCM) was dried by stirring overnight with anhydrous $MgSO_4$, and toluene was distilled under dinitrogen from sodium. $[Re(bipy)(CO)_3Br]$,[23] 5-(hydroxymethyl)-2,2′-bipyridine,[24] and 5-(aminomethyl)-2,2′-bipyridine[25] were prepared according to literature procedures. A hydroxylamine-reduced silver colloid was prepared from $AgNO_3$ (99.9999% Sigma-Aldrich) and hydroxylamine hydrochloride (99.999% Sigma-Aldrich) according to the method described by Leopold et al.[26]

Raman Experiments. Typically, 0.01 mol dm^{-3} aqueous KBr (20 μL) was added to the aqueous colloid (160 μL), followed by the analyte (40 μL) as a solution in acetone (HPLC grade, J. T. Baker) and 0.1 mol dm^{-3} aqueous $MgSO_4$ (40 μL) to aggregate the colloid. Dilutions of the analyte were with doubly deionized (DDI) water. For the experiments run at 785 nm, the samples were autofocused in a 96-well plate by the instrument and then accumulated for 3 × 10 s. For the samples run at 532 nm, a 20 μL drop of the prepared mixture was placed on a glass slide covered with aluminum foil, manually focused under the 4× objective lens, and irradiated for 10 × 1 s. Spectra were manipulated using the *Grams/AI* program.[27]

Calculations. These were run using the *Gaussian03* program.[28] Geometry optimization and calculation of Raman frequencies were carried out using density functional theory (DFT) at the B3LYP level of theory.[29] For C, H, N, and O atoms, the 6-31G basis set was used, while the Lanl2 effective core potential with 2-double-ζ (Lanl2DZ) was used for Re, Br, and S atoms;[30] the first five highest occupied molecular (HOMO) and lowest unoccupied molecular (LUMO) orbitals were calculated.

Synthesis. *(2,2′-Bipyridin-5-ylmethyl)-5-(1,2-dithiolan-3-yl)pentanoate (**L1**).* 5-(Hydroxymethyl)-2,2′-bipyridine (0.186 g, 1.00 mmol) and (±)-1,2-dithiolane-3-pentanoic acid (0.2472 g, 1.2 mmol) were dissolved in dry DCM (30 cm^3) and stirred for 45 min at 0 °C under dinitrogen. Then dicyclohexylcarbodiimide (DCC; 0.309 g, 1.5 mmol) and 4-(dimethylamino)pyridine (DMAP; 0.367 g, 0.30 mmol) in dry DCM (15 cm^3) were added and stirred for 1 h at 0 °C and subsequently at room temperature for 36 h. The resulting pale-yellow solution was washed with water (3 × 30 cm^3), the organic residues were dried over anhydrous $MgSO_4$, and the solvent was removed at reduced pressure. The crude yellow solid was purified by silica column chromatography (eluent: 59:39:2 hexane/ethyl acetate/triethylamine), collecting the first major fraction. Yield: 0.21 g, 56%. ^{1}H NMR ($CDCl_3$, 300 MHz): δ_H 1.49 (2H, m, 11), 1.70 (4H, m, 10,12), 1.88 (1H, m, 14), 2.41 (3H, m, 9,14), 3.13 (2H, m, 15), 3.55 (1H, m, 13), 5.19 (2H, s, 7), 7.33 (1H, dd, *J* = 7.5 and 4.9 Hz, 5′), 7.83 (2H, m, 4,4′), 8.40 (1H, d, *J* = 8.1 Hz, 3), 8.41 (1H, d, *J* = 8.4 Hz, 3′), 8.70 (2H, m, 6,6′). ^{13}C NMR ($CDCl_3$, 75 MHz): δ_C 25.0, 25.4, 34.4, 34.9, 38.9, 40.6, 56.7, 63.9, 121.5, 121.6, 124.3, 132.1, 137.4, 149.4, 149.5, 149.6, 156.1, 156.5, 173.5. ES-MS: 375.2 $[M]^+$. Elem anal. Found (calcd) for $C_{19}H_{22}O_2N_2S_2 \cdot 0.25H_2O$: C, 60.13 (60.21); H, 6.15 (5.91); N, 7.58 (7.39).

*N-(2,2′-Bipyridin-5-ylmethyl)-5-(1,2-dithiolan-3-yl)pentanamide (**L2**).* **L2** was prepared according to the procedure for **L1** using 5-(aminomethyl)-2,2′-bipyridine (0.186 g, 1.00 mmol). The crude yellow product was purified by recrystallization twice from a hot toluene/methanol/acetone mixture (60:20:20, v/v). Yield: 0.48 g, 66%. ^{1}H NMR ($CDCl_3$, 300 MHz): δ_H 1.43−1.51 (2H, m, 11), 1.65−1.72 (4H, m, 10,12), 1.89 (1H, m, 14), 2.25 (2H, t, *J* = 7.6 Hz, 9), 2.43 (1H, m, 14), 3.07−3.18 (2H, m, 15), 3.56 (1H, m, 13), 4.51 (2H, d, *J* = 5.7 Hz, 7), 5.93 (1H, br, *N*H), 7.30 (1H, dd, *J* = 7.4 and 4.8 Hz, 5′), 7.75 (1H, d, *J* = 8.2 Hz, 4), 7.81 (1H, t, *J* = 7.8 Hz, 4′), 8.35 (1H, d, *J* = 8.2 Hz, 3), 8.36 (1H, d, *J* = 8.0 Hz, 3′), 8.58 (1H, s, 6), 8.67 (1H, d, *J* = 4.8 Hz, 6′). ^{13}C NMR ($CDCl_3$, 75 MHz): δ_C 25.3, 33.9, 34.6, 36.3, 38.4, 40.2, and 40.8 (CH_2), 56.3 (C13), 121.0 (C3/3′), 121.1 (C3/3′), 123.7 (C5′), 134.1 (Q), 136.5 (C4/4′), 136.9 (C4/4′), 148.6 (C6/6′), 149.2 (C6/6′), 155.5 (Q), 155.8 (Q), 172.8 (C═O). EI-MS: 373.1 $[M]^+$. Elem anal. Found (calcd) for $C_{19}H_{23}ON_3S_2 \cdot$acetone$\cdot 0.1MgSO_4$: C, 59.46 (59.56); H, 6.88 (6.59); N, 9.19 (9.47); S, 15.50 (15.18).

*Ethyl-5-(1,2-dithiolan-3-yl)pentanoate (**L3**).* **L3** was prepared according to the procedure for **L1** using a large excess of ethanol. Yield: 34.2 mg, 30%. ^{1}H NMR ($CDCl_3$, 300 MHz): δ_H 1.25 (3H, t, *J* = 7.2 Hz, 1), 1.41−1.49 (2H, m, 6), 1.60−1.73 (4H, m, 5,7), 1.90 (1H, m, 9a), 2.30 (2H, t, *J* = 7.3 Hz, 4) 2.45 (1H, m, 9b), 3.06−3.21 (2H, m, 10), 3.56 (1H, m, 8), 4.12 (2H, q, *J* = 7.1 Hz, 2). ^{13}C NMR ($CDCl_3$, 75 MHz): δ_C 14.2 (CH_3), 24.6, 28.7, 34.1, 34.6, 38.4, 40.2, 56.3 (CH), 60.2 (CH_2O), 173.4 (C═O). EI-MS: *m*/*z* 234.07 $[M]^+$. Elem anal. Found (calcd) for $C_{10}H_{18}O_2S_2 \cdot 0.3$acetone: C, 51.82 (51.99); H, 7.95 (7.93); N, 0.01 (0.00); S, 25.97 (25.47). IR (KBr disk): 1734.2 (C═O stretch).

*[Re(**L1**)(CO)$_3$Br].* To [Re(CO)$_5$Br] (0.049 g, 0.12 mmol) in refluxing dry toluene (50 cm^3) was added **L1** (45.3 mg, 0.12 mmol) dissolved in dry toluene (25 cm^3), and the mixture was refluxed for 18 h under an N_2 atmosphere. The volume of the solvent was then reduced to ∼5 cm^3, causing precipitation of a yellow solid, which was filtered under vacuum, washed with diethyl ether, and dried at 60 °C. Yield: 67.1 mg, 77%. ^{1}H NMR [$(CD_3)_2CO$]: δ_H 1.48 (2H, m, 11), 1.60−1.78 (4H, m, 10,12), 1.90 (1H, m, 14), 2.43−2.50 (3H, m, 9,14), 3.07−3.19 (2H, m, 15), 3.59−3.62 (1H, m, 13), 5.42 (2H, s, 7), 7.79 (1H, dd, *J* = 7.7 and 5.5 Hz, 5′), 8.33 (2H, m, 4,4′), 8.70 (1H, d, *J* = 8.2 Hz, 3), 8.71 (1H, d, *J* = 8.5 Hz, 3′), 9.13 (1H, d, *J* = 5.5 Hz, 6), 9.15 (1H, s, 6′). ^{13}C NMR [126 MHz, $(CD_3)_2CO$]: δ_C 26.4, 35.3, 36.3, 40.1, 41.9, 58.11, 58.13, 63.9, 125.7, 126.1, 129.5, 138.8, 141.1, 141.7, 154.0, 155.1, 157.2, 157.4, 174.3 (C═O), 191.1, 199.4 (3C≡O). ES-MS: *m*/*z* 747 $[M + Na]^+$, 645 $[M - Br]^+$, 723 $[M - H]^-$. Elem anal. Found (calcd) for $ReC_{22}H_{22}O_5N_2S_2Br \cdot 0.4$diethyl ether: C, 37.12 (37.58); H, 3.51 (3.47); N, 3.50 (3.71); S, 8.05 (8.50). IR (KBr disk): 1739.3 (C═O), 1902.4, 2021.5 (3ReC=O).

*[Re(**L2**)(CO)$_3$Br].* [Re(**L2**)(CO)$_3$Br] was prepared according to the procedure for [Re(**L1**)(CO)$_3$Br]. Yield: 36%. ^{1}H NMR [500 MHz, $(CD_3)_2O$]: δ_H 1.43−1.49 (2H, m, 11), 1.59−1.76 (4H, m, 10,12), 1.89 (1H, m, 14), 2.31 (2H, t, *J* = 7.4 Hz, 9), 2.46 (1H, m, 14), 3.05−3.20 (2H, m, 15), 3.60 (1H, m, 13), 4.65 (2H, d, *J* = 6.2 Hz, 7), 7.77 (1H, dd, *J* = 7.6 and 5.5 Hz, 5′), 7.92 (1H, br, *N*H), 8.22 (1H, d, *J* = 8.4 Hz, 4), 8.31 (1H, t, *J* = 7.9 Hz, 4′), 8.63 (1H, d, *J* = 8.2 Hz, 3), 8.66 (1H, d, *J* = 8.2 Hz, 3′), 9.01 (1H, s, 6), 9.11 (1H, d, *J* = 5.5 Hz, 6′). ^{13}C NMR [126 MHz, $(CD_3)_2O$]: δ_C 26.6, 35.8, 36.8, 39.5, 41.0, 41.3, 57.6, 125.0, 125.1, 128.6, 140.2, 141.0, 141.6, 153.2, 154.4, 154.5, 155.7, 157.0, 174.0 (C═O), 190.6, 198.8 (3C≡O). ES-MS: 644 $[M - Br^-]^+$, 722 $[M - H]^-$. Elem anal. Found (calcd) for $ReC_{22}H_{23}O_4N_3BrS_2 \cdot 0.5$diethyl ether$\cdot 2H_2O$: C, 36.13 (36.18); H, 4.32 (4.05); N, 4.96 (5.27); S, 7.67 (8.05). IR (KBr disk): 1652.1 (C═O stretch), 1916.1, 2022.5 (3ReC═O stretch).

RESULTS

Synthesis and Characterization. The tethering of photoactivated metal complexes to gold and silver surfaces has attracted much attention in recent years, usually this is achieved through an alkyl thiol to form a SAM.[10] In this study, silver nanoparticles were selected over the more commonly studied gold particles because of the high enhancement factors that they provide in the SERS study undertaken. However, silver thiol bonds are more labile than the analogous gold surfaces, and so a chelating dithiolate was used to avoid the possibility of the complex being released from the surface. The commercially available thioctic acid [5-(1,2-dithiolan-3-yl)pentanoic acid] was selected for this purpose because it can be readily modified to provide a functionalized SAM.[31]

L1 and the equivalent amide **L2** were produced from 5-(hydroxymethyl)-2,2′-bipridine and 5-(aminomethyl)-2,2′-bipyridine, respectively, by a DCC coupling with thioctic acid, followed by purification on silica in the case of **L1** or recrystallization for **L2**, giving moderate yields in each case. Some evidence of the deesterification of **L1** was observed on silica, causing a lower than anticipated yield. The ethyl ester of thioctic acid, **L3**, was produced in the same way, although with a comparatively low yield presumably also because of deesterification during purification (Scheme 1). Despite repeated attempts to purify the ligands further and prolonged drying under vacuum, all three compounds were observed to retain solvent, which was evident in both the NMR spectra and elemental analyses.

The facial tricarbonylrhenium(I) complexes [Re(**L1**)(CO)$_3$Br] and [Re(**L2**)(CO)$_3$Br] were isolated by the reaction of ligands **L1** and **L2** with Re(CO)$_5$Br in toluene[23] and the identities of the products confirmed by ^{1}H NMR spectroscopy, CHN analysis, and electrospray mass spectrometry, although the complexes were observed to retain solvent. The UV/vis spectra show typical absorption bands associated with this type of complex (Table 1).[4,21,32] For both the ester and amide complexes, [Re(**L1**)(CO)$_3$Br] and [Re(**L2**)(CO)$_3$Br], the positions of the UV/vis absorptions are not significantly different from those of the

Scheme 1[a]

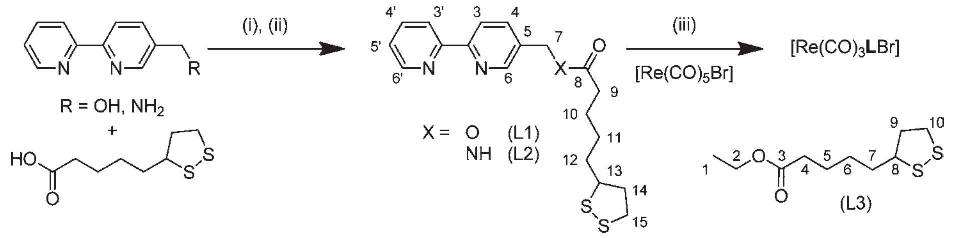

[a] (i) Dry DCM, 0 °C, N_2; (ii) DCC, DMAP; (iii) dry toluene, reflux, N_2.

Table 1. Photophysical Properties of the Isolated Rhenium(I) Complexes

	absorption, λ_{max}/nm (ε/M^{-1}cm^{-1})				emission	
complex	LC		MLCT		λ_{max}/nm	Φ_{em}
[Re(bipy)(CO)$_3$Br]	244 (18 500)	292 (12 500)	315 (9800)	366 (2320)	609	7.8×10^{-3}
[Re(**L1**)(CO)$_3$Br]	239 (20 500)	287 (15 800)	312 (sh)	369 (3000)	618	2.08×10^{-3}
[Re(**L2**)(CO)$_3$Br]	244 (21 500)	291 (15 500)	317 (10 600)	368 (2990)	610	4.16×10^{-3}

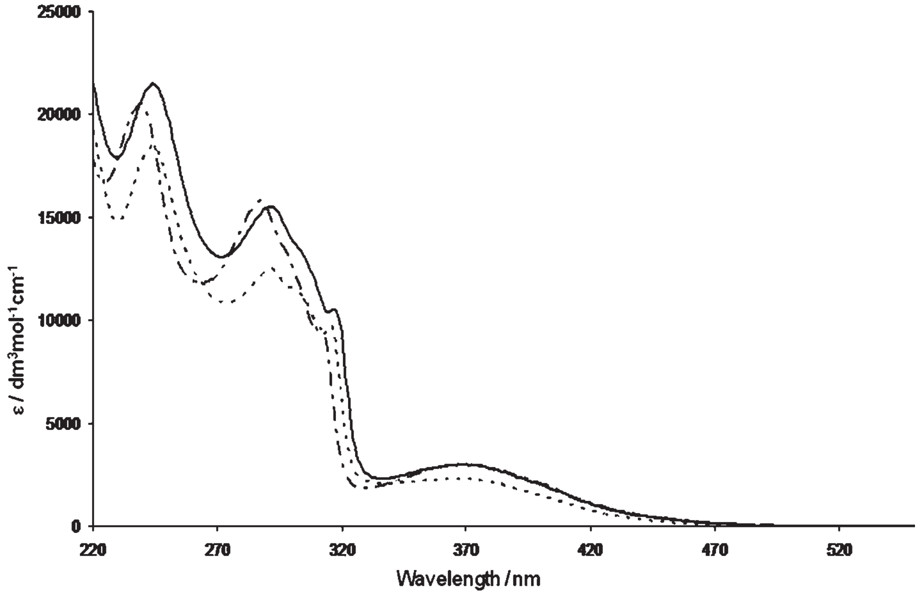

Figure 2. UV/vis absorption spectra of [Re(bipy)(CO)$_3$Br] (- - -), [Re(**L1**)(CO)$_3$Br] (•••), and [Re(**L2**)(CO)$_3$Br] (—).

reference complex [Re(CO)$_3$(bipy)Br] with a marginal red shift of the MLCT and ligand-centered bands (Figure 2), while the absorptions themselves were observed to be a little more intense. The presence of the electron-withdrawing carbonyl groups in the ester and amide groups does not cause a significant red shift in the transitions, as observed in our previously reported rhenium complexes,[20,21] where there are no methylene groups isolating the bipyridyl ring from the appended electron-withdrawing carbonyl function.

DFT descriptions of the charge-transfer electronic excited states, including those of rhenium(I), have recently been extensively reviewed by Vlček et al.[33] DFT calculations on [Re(**L1**)(CO)$_3$Br] and [Re(**L2**)(CO)$_3$Br] suggest that the HOMO is a mixed metal—ligand orbital with a considerable electron density residing on the Br and C atoms of the carbonyl groups in addition to the rhenium center (Figure 3), consistent with the respective π-donating and -accepting behavior of these groups. For both complexes, the HOMO is at around −5.6 eV, but there are also other orbitals at very similar energies: one again centered on the metal, Br, and CO ligands and the other centered on the S atoms of the alkyl chain on the bipy ligand. As would be expected, the LUMOs (at around −2.8 eV in each case) are mostly centered on the bipyridine unit. This matches well with the lowest energy transition observed in the UV/vis spectrum, suggesting that it has a metal—ligand-to-ligand charge-transfer character. These observations are in agreement with calculations carried out on similar molecules, [Re(CO)$_3$(bipy)Cl],[34,35] [Re(CO)$_3$(2,2′-biquinoline)Cl],[36] and [Re(CO)$_3$(dppt)Cl] (dppt = 5,6-diphenyl-3-(2-pyridyl)-1,2,4-trazine),[37] where a mixed metal—ligand (CO and Cl) HOMO and bipy-centered

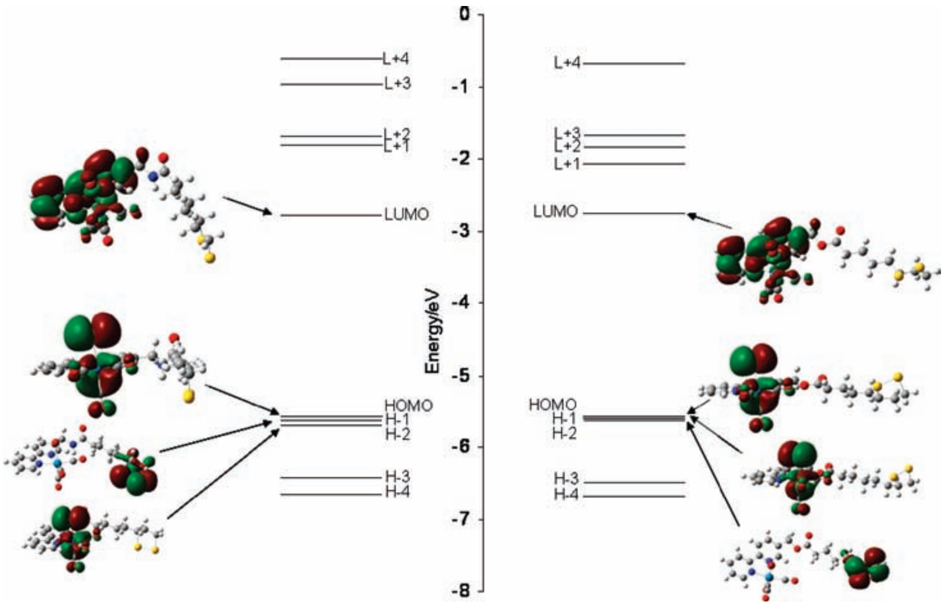

Figure 3. DFT calculation and pictorial representation of frontier orbitals of $[\mathrm{Re}(\mathbf{L1})(\mathrm{CO})_3\mathrm{Br}]$ (left) and $[\mathrm{Re}(\mathbf{L2})(\mathrm{CO})_3\mathrm{Br}]$ (right).

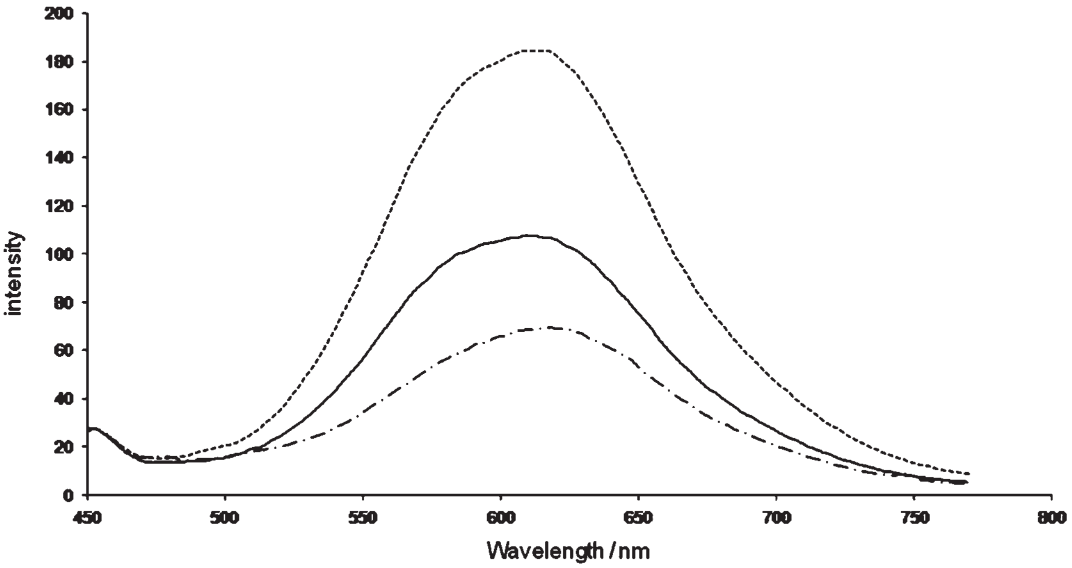

Figure 4. Emission spectra of $[\mathrm{Re(bipy)(CO)_3Br}]$ (- - -), $[\mathrm{Re}(\mathbf{L1})(\mathrm{CO})_3\mathrm{Br}]$ (•-•), and $[\mathrm{Re}(\mathbf{L2})(\mathrm{CO})_3\mathrm{Br}]$ (—) in aerated acetonitrile, in a 1 cm cuvette adjusted to an absorption of 0.1 at 400 nm and excited at 400 nm.

LUMO were reported. The energy gaps between the HOMO and LUMO observed in this study were 2.80 and 2.83 eV, respectively, for $[\mathrm{Re(CO)_3}(\mathbf{L1})\mathrm{Br}]$ and $[\mathrm{Re(CO)_3}(\mathbf{L2})\mathrm{Br}]$, clearly indicating the similarity of the two complexes.

Both $[\mathrm{Re}(\mathbf{L1})(\mathrm{CO})_3\mathrm{Br}]$ and $[\mathrm{Re}(\mathbf{L2})(\mathrm{CO})_3\mathrm{Br}]$ demonstrate the anticipated phosphorescence, having slightly lower emission quantum yields in an aerated solution than the reference complex $[\mathrm{Re(bipy)(CO)_3Br}]$ (Figure 4). With the methylene spacer attached to the chromophore, it is noticeable that the luminescence is significantly greater than that in our previously reported complexes,[20,21] where a large red shift and quenching in the luminescence with respect to the standard reference compound were observed,[22] again attributed to the direct attachment of an electron-withdrawing amide group to the diimine group.

Raman Spectroscopy. The protocol followed for the collection of Raman spectra was the result of optimization of both the solvent and aggregating conditions. A total of 20 μL of 0.01 mol dm^{-3} KBr was added to the colloid prior to the analyte to replace the existing Cl ions on the surface of the colloid with Br ions without causing its aggregation. This was to allow experiments aimed at detection of the putative Ag−S bonds (∼234 cm^{-1} for alkanethiols)[38] without interference from the strong Ag−Cl bond (∼240 cm^{-1}) found in an "as-prepared" hydroxylamine-reduced colloid; the Ag−Br bond lies at ∼160 cm^{-1}. The sol was subsequently aggregated by the addition of aqueous magnesium sulfate, following a protocol determined experimentally to maximize the SERS intensity. Both the ligands and complexes described above were analyzed by this procedure. To aid

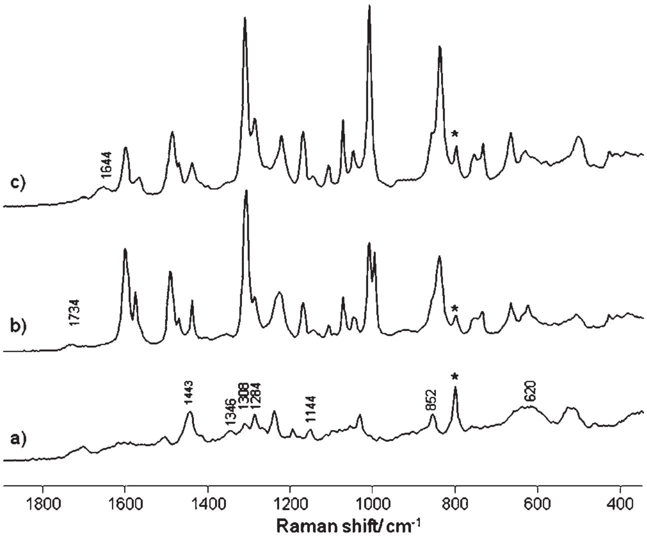

Figure 5. 160 μL of silver colloid with 20 μL of 0.01 mol dm^{-3} KBr(aq), 40 μL of 0.1 mol dm^{-3} $MgSO_4$(aq), and 40 μL of 5 × 10^{-4} mol dm^{-3} acetone solutions of (a) **L3**, (b) **L1**, (c) and **L2**; excited at 785 nm (* = acetone).

assignment of the bands in the rather complex spectra, some precursors of the isolated complexes were also analyzed. Initially, spectra of thioctic acid solutions were recorded with the expectation that this would help to identify the signals relating to the disulfide group and the aliphatic chain; however, the compound gave very low intensity spectra, presumably because of interference by the carboxylate group. To overcome this difficulty, the ethyl ester derivative of thioctic acid (**L3**) was prepared as a model compound that would not dissociate and would give bands associated with the "surface tether".

Ligand Behavior. An initial comparison of the ligand spectra (**L1** and **L2**) and the ethyl ester of thioctic acid (**L3**) was attempted (Figure 5). Through excitation at 785 nm, it was hoped that the bipyridyl chromophore would not be significantly resonance-enhanced, providing an opportunity to observe the signals arising from the alkyl chain also. The spectra of **L1** and **L2** are, however, still dominated by the large bipyridine bands, but it is also possible to detect the bands arising from the tether in all three spectra, despite masking by the signals attributed to the bipyridine group. Peaks at 620 (br), 852 (which appears as a shoulder in bipyridine-containing samples), 1144, 1284, 1308, 1346 (a shoulder in bipyridine-containing samples), and 1443 cm^{-1} appear in both the simple ester spectrum (**L3**) and those of **L1** and **L2**. It is also possible to observe weak carbonyl stretching bands at 1644 and 1734 cm^{-1} for **L2** and **L1**, respectively, that compare favorably with the bands in the IR spectra (KBr disks), appearing at 1637 and 1734 cm^{-1}. Additionally, evidence for the presence of a Ag—S bond was observed in the spectra of both complexes [Re(**L1**)$(CO)_3$Br] and [Re(**L2**)$(CO)_3$Br] and also **L2** (very weak), excited at 785 nm (not shown). A small peak is observed at 236—238 cm^{-1}, which would be consistent with literature reports for a metal—sulfur stretching mode, although metal—nitrogen stretches can also be found in this region.[39] However, this band is not observed for the ligand **L1** at this wavelength, and neither the ligands, nor the complexes described subsequently, display this peak when excited at 532 nm.

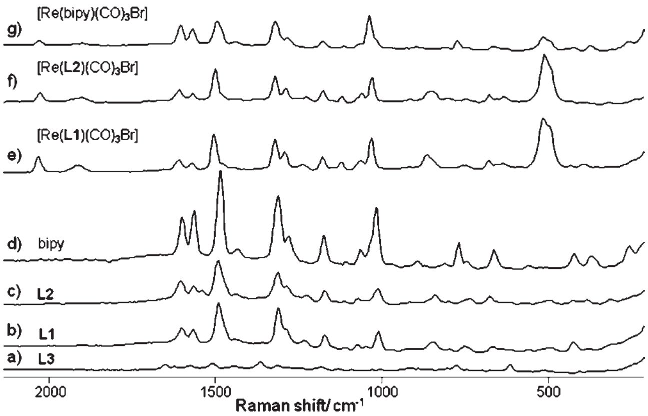

Figure 6. Raman spectra of 160 μL of silver colloid with 20 μL of 0.01 mol dm^{-3} KBr(aq), 40 μL of 0.1 mol dm^{-3} $MgSO_4$(aq), and 40 μL of acetone solutions of (a) 1 × 10^{-5} mol dm^{-3} **L3**, (b) 1 × 10^{-5} mol dm^{-3} **L1**, (c) 1 × 10^{-5} mol dm^{-3} **L2**, (d) 1 × 10^{-5} mol dm^{-3} bipy, (e) 2.5 × 10^{-5} mol dm^{-3} [Re(**L1**)$(CO)_3$Br], (f) 2.5 × 10^{-5} mol dm^{-3} [Re(**L2**)$(CO)_3$Br], and (g) [Re(bipy)$(CO)_3$Br]; excited at 532 nm.

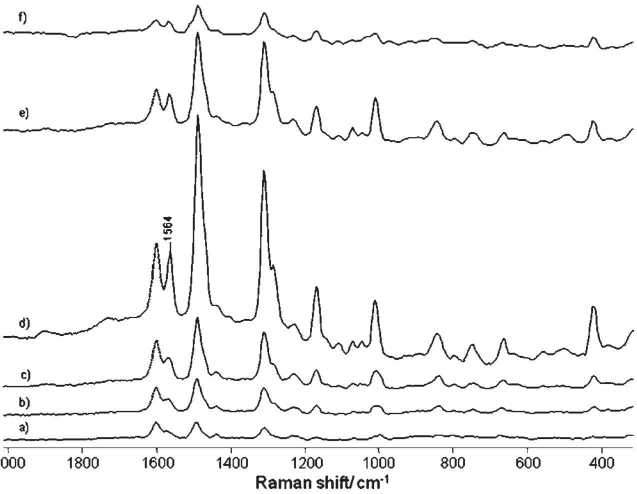

Figure 7. Concentration dependence of the SERRS spectrum of **L1**. Experimental conditions as in Figure 5 except that the final concentrations are (a) 1.54 × 10^{-4} mol dm^{-3}, (b) 3.08 × 10^{-5} mol dm^{-3}, (c) 1.54 × 10^{-5} mol dm^{-3}, (d) 3.08 × 10^{-6} mol dm^{-3}, (e) 1.54 × 10^{-6} mol dm^{-3}, and (f) 3.08 × 10^{-7} mol dm^{-3}.

The spectra of 2,2′-bipyridine (bipy), **L1**, and **L2** excited at 532 nm (Figure 6b,c) are consistent with the spectra recorded at 785 nm (Figure 5). It was also observed that at this wavelength the contributions to the observed spectra of **L1** and **L2** do not contain a significant contribution from the surface tether (Figure 6a). Previous reports have noted the similarity between the spectrum of bipy and that of $[Ag(bipy)_2]^+$ and have been attributed to chelation of the two bipy N atoms with the silver surface.[40,41] A comparison of the bipy spectrum (Figure 6d) with those of **L1** and **L2** shows that the spectra of these two complexes are dominated by bipyridine peaks, although the relative intensity of the peaks is slightly different for the peaks at 1564 and 1600 cm^{-1}, which are assigned as C=C stretching modes,[40] presumably because of the effects of substitution on the aromatic ring or orientation on the surface.

A study of the concentration dependence of the SERS spectra of **L1** (Figure 7) shows that, at higher concentrations of the ligand, the spectrum has a relatively low intensity, and a small

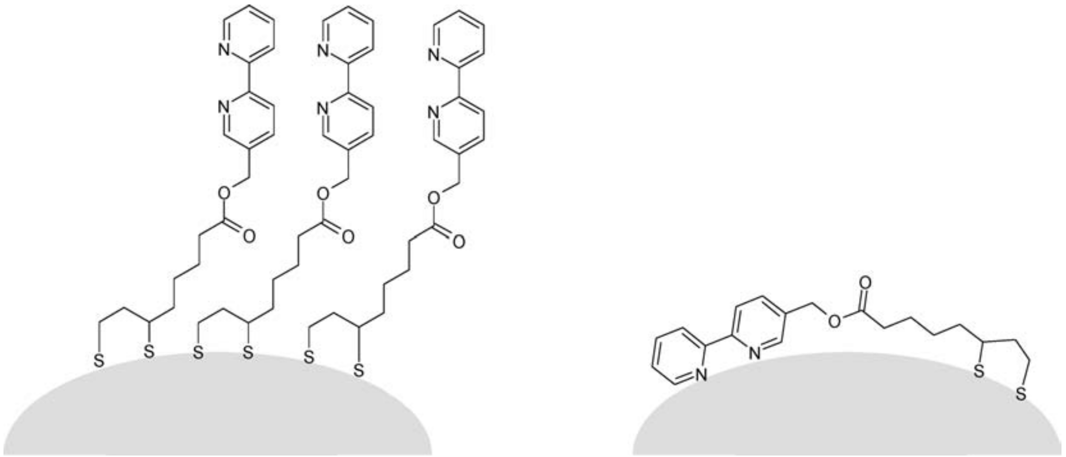

Figure 8. Schematic representation of the effect of the concentration on the surface binding behavior of **L1** with silver nanoparticles.

shoulder at 1574 cm^{-1} can be observed on the 1602 cm^{-1} peak. As the sample is diluted, the intensity of the peaks across the spectrum increase; in particular, the shoulder emerges as a separate peak at 1564 cm^{-1}. At low concentrations, the spectra recorded are reminiscent of the spectra of the bipyridine complexes, where a peak at approximately 1564 cm^{-1} has previously been assigned as a C=C stretching mode of bipyridine.[40] A number of properties could potentially be responsible for this given the complexity of the system involved. Assuming that the sample is already fully aggregated with the addition of the magnesium sulfate solution, this behavior can be rationalized by assuming that the disulfide group will have a higher affinity for the silver surface than the bipy N atoms, so at high concentration, the bipyridine part of the molecule is forced to "stand up" on the surface (Figure 8). At lower concentration, with partial surface coverage, there will be sufficient room on the surface for the bipyridine part to collapse down, giving a spectrum more representative of free bipyridine. Once a maximum sample signal is reached (for the ester ligand **L1**, this occurred at an overall concentration of close to 2×10^{-6} mol dm^{-3}), the intensity of the signals begins to decrease again, presumably because of the submonolayer coverage on the silver surface. Similar behavior is also observed for **L2** within the same concentration range; however, in this case, both peaks at 1605 and 1565 cm^{-1} remain approximately equal in relative intensity at each concentration tested (data not shown).

Complex Behavior. A comparison between **L1** and its rhenium complex $[Re(\mathbf{L1})(CO)_3Br]$, excited at 532 nm (Figure 9), indicated striking differences between the two spectra. For the complex, there are additional bands: a broad band at 1909 cm^{-1}, a sharp band at 2028 cm^{-1}, and an intense band at 510 cm^{-1}. The first two bands are attributed to the stretching of the coordinated carbonyl ligands. The band at 2028 cm^{-1} is attributed to the in-phase symmetric mode of all three carbonyls and is consistent with both the literature[17,18,34,42] and our calculations (although these place the frequency of the vibration slightly higher), while the 1909 cm^{-1} band is likely to be an antisymmetric ν(CO) in keeping with the assignments made by Bredenbeck et al.[43] These bands are also observed in the solid-state IR spectrum of the same complex. The band at 510 cm^{-1} is assigned to Re—CO stretching.[17] At a lower concentration of the complex, the small shoulder observed on this band splits into a second peak. This is likely to relate to the difference between the C atoms being trans to either a N or Br atom, respectively.

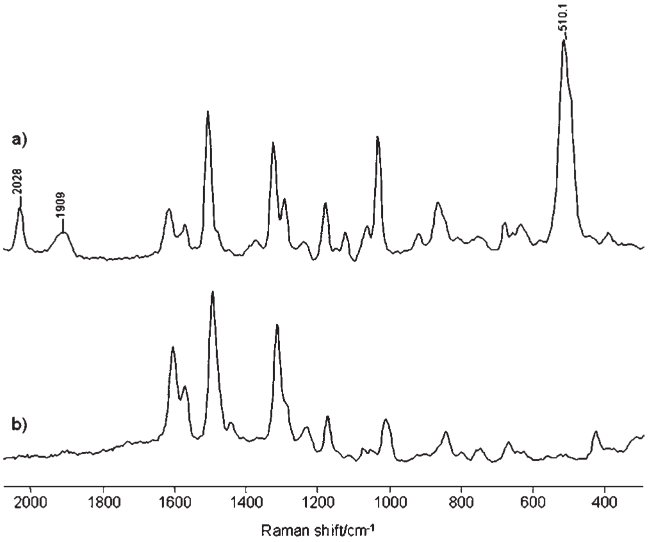

Figure 9. 160 μL of silver colloid with 20 μL of 0.01 mol dm^{-3} KBr(aq), 40 μL of 0.1 mol dm^{-3} $MgSO_4$(aq), and 40 μL of acetone solutions of (a) 5×10^{-5} mol dm^{-3} $[Re(\mathbf{L1})(CO)_3Br]$ and (b) 1×10^{-4} mol dm^{-3} **L1**; excited at 532 nm.

Various bands attributed to the bipyridine moiety also appear to have shifted slightly in their position upon complexation to rhenium. A similar situation is observed with the amide derivatives **L2** and $[Re(\mathbf{L2})(CO)_3Br]$ (Figure 6).

A concentration dependence is observed for both the complexes $[Re(CO)_3(\mathbf{L1})Br]$ and $[Re(CO)_3(\mathbf{L2})Br]$ (Figures S1 and S2 in the Supporting Information, respectively), whereby the maximum signal is observed at a relatively low concentration (3.8×10^{-6} M for both) before, at higher concentrations, a dramatic decrease in the signal intensity is observed, consistent with the rhenium complex lifting off the surface but being retained in close proximity because of the thiol-tethered ligands. This is presumably due to a phenomenon similar to that of the ligand, whereby the signals of the bipyridine moiety are further enhanced as the surface crowding is reduced, and this part of the complex will have a greater opportunity to be in close proximity to the silver surface.

Figure 10 compares the spectra of $[Re(\mathbf{L2})(CO)_3Br]$, excited at 532 and 785 nm. These spectra have been scaled to allow a direct comparison of the bands and to emphasize the similarity in

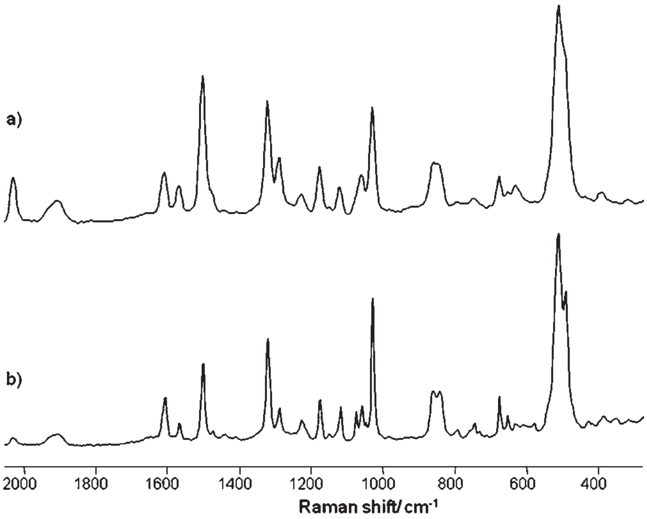

Figure 10. 160 μL of silver colloid with 20 μL of 0.01 mol dm^{-3} KBr(aq), 40 μL of 0.1 mol dm^{-3} MgSO$_4$(aq), and 40 μL of a 2.5 × 10^{-5} mol dm^{-3} acetone solution of [**Re**(**L2**)(CO)$_3$Br], excited at (a) 532 nm and (b) 785 nm (intensity not to scale).

the positions and relative intensities of the bands observed at both excitation wavelengths; they do not show the difference in the absolute intensities. The 532 nm excitation appeared to give higher intensity spectra than those under 785 nm irradiation, although any variation between the output strength and detection response of the two instruments used in the study could not be taken into consideration because of technical difficulties. A weak resonance enhancement of the signals attributed to the rhenium(I) chromophore, when excited at a wavelength close to the MLCT absorption (Figure 2), would be anticipated. However, the similarity of the spectra recorded at both 532 and 785 nm suggests that, even at these excitation wavelengths, there is an enhancement, which results in the same pattern of relative band intensities in the chromophore. It is proposed that this could arise from a surface plasmon emission at higher energy than the initial irradiation as a result of multiple photon absorptions into the silver plasmon band of the aggregated colloid, albeit with a reduced overall scattering intensity. It is also striking that the bands due to the CO vibrations in the complex have intensity comparable to those of the bipy ligand. This is presumably a consequence of the delocalized nature of the orbitals involved in the MLCT transition.[44] As shown in Figure 3, the terminal orbital is predominantly bipy-based but is strongly delocalized over the metal center. Similarly, the metal orbital, which acts as the source of the electron, will be strongly mixed with those of the coordinated CO. In this case, the parts of the complex that are perturbed during the MLCT transition and are therefore, for these purposes, parts of the chromophore include not only the bipy ligands but also the CO ligands, as has been previously demonstrated by Schoonover et al. using time-resolved vibrational studies.[45] This is useful for our overall modular approach because it shows that ligands attached to the metal center can display SERRS scattering by coupling through the metal center to other strongly chromophoric ligands.

Using SERS, rather than resonance Raman, to examine luminescent complexes such [Re(**L1**)(CO)$_3$Br] and [Re(**L2**)(CO)$_3$Br] means that the luminescence should be quenched by the silver nanoparticles employed.[17] Observations made by emission spectroscopy, irradiated at 400 nm, confirm that, at higher concentrations assumed to be above that required for full surface coverage, phosphorescent species remain in solution to give a relatively high background level of emission. At lower concentrations of [Re(**L1**)(CO)$_3$Br], the emission intensity decreases in the presence of silver colloid. This appears to be consistent with the concentration below which the monolayer is no longer saturated, and all of the transition-metal complexes are surface-bound, thereby quenching the emission.

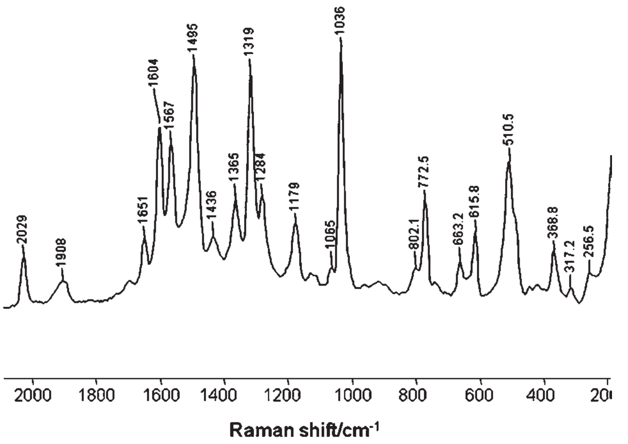

Figure 11. 160 μL of silver colloid with 20 μL of 0.01 mol dm^{-3} KBr(aq), 40 μL of 0.1 mol dm^{-3} MgSO$_4$(aq), and 40 μL of a 1 × 10^{-4} mol dm^{-3} acetone solution of [Re(**bipy**)(CO)$_3$Br], excited at 532 nm.

Previous reports have suggested that the SERS spectrum of [Re(bipy)(CO)$_3$Br] cannot be obtained because of the lack of any functionality to attach the complex to the surface.[17] However, using the protocol described within this study, it is possible to obtain a convincing spectrum for this molecule, with the observation of the characteristic Re—CO and C═O stretches (Figure 11) as seen in complexes [Re(**L1**)(CO)$_3$Br] and [Re(**L2**)(CO)$_3$Br]. It was, however, observed that the complex did not self-aggregate in the presence of colloid and after standing for 1.5 h (50 μL of a 1 × 10^{-3} mol dm^{-3} solution of [Re(bipy)(CO)$_3$Br] in acetone and 200—1000 μL of colloid made up to 3000 μL with DDI water), indicating the necessity of the salt to promote aggregation. It should be noted that the minimum concentration of analyte that is needed to obtain a satisfactory spectrum is higher than that for analogous complexes containing the disulfide chain.

The evidence suggests that the tether parts of complexes [Re(**L1**)(CO)$_3$Br] and [Re(**L2**)(CO)$_3$Br] do play an important role in keeping the complex close to the surface. For the simple [Re(bipy)(CO)$_3$Br] complex, while it is possible to observe a spectrum at a final concentration of 1.5 × 10^{-5} mol dm^{-3}, the intensity of the spectrum falls off quickly below this, while the intensity of the analogous complex with the disulfide chain attached only begins to decrease significantly around final concentrations of 7.7 × 10^{-6} mol dm^{-3} for [Re(CO)$_3$(**L1**)Br] and 7.7 × 10^{-7} mol dm^{-3} for [Re(CO)$_3$(**L2**)Br]. As a result, it would appear that the formation of Ag—S bonds with the disulfide thioctic acid derivative might be crucial in the persistence of Raman signals at such low concentrations.

■ CONCLUSIONS

Within this study, we have attempted to explore the interactions of dithiolated bipyridine systems on silver nanoparticles using SE(R)RS, both with and without luminescent *fac*-carbonylrhenium groups. It has become apparent that the surface concentration of the sample is extremely important; for all of the systems studied, three distinct phases appear to be in operation. At very low concentration, both the thiol and diimine groups are bound to the surface, while as the concentration increases, the bipyridine lifts off the surface and finally there is an increase in the luminescence background as the surface has been completely covered and excess reagent is present in solution. Given this switching behavior, this paper illustrates that the rhenium-based absorptions are excited through irradiation at 532 nm, presumably via the influence of the aggregated silver colloid. It is therefore acting as a suitable sensitizer to amplify a surface-enhanced Raman signal, i.e., act as a transducer. It is hoped that in future studies the excitation wavelength can be used to address specifically the alkyl chain, the bipyridine, or even the rhenium-centered MLCT part of the molecule because this should provide a direct route to switching output signals from the various parts of the molecule, allowing interrogation of both the chromophore and other appended components. From a synthetic point of view, the flexibility of the rhenium tricarbonyl motif is an advantage; it is envisaged that this system will provide a versatile starting point on which to build further functionality (Figure 1) using traditional coordination chemistry. We are currently examining the behavior of the system with the in situ replacement of the bromide with nitrogen-based ligands, which ultimately can be appended to enzyme metabolites for consideration as probes of biological systems.

■ ASSOCIATED CONTENT

S Supporting Information. Concentration-dependent studies for complexes $[\mathrm{Re(CO)_3}(\mathbf{L1})\mathrm{Br}]$ and $[\mathrm{Re(CO)_3}(\mathbf{L2})\mathrm{Br}]$ (Figures S1 and S2), Cartesian coordinates of the optimized structures, and MOL files for the results from DFT-optimized studies. This material is available free of charge via the Internet at http://pubs.acs.org.

■ AUTHOR INFORMATION

Corresponding Author

*E-mail: n.fletcher@qub.ac.uk. Telephone: +44 (0)28 9097 5479.

■ ACKNOWLEDGMENT

The authors are thankful for the assistance of Dr. M. Migaud in the conception of the project and DELNI for a Ph.D. studentship for H.J.M. Dr. R. Oakes is kindly acknowledged for her help with the DFT calculations.

■ REFERENCES

(1) Kumar, A.; Sun, S.-S.; Lees, A. J. *Top. Organomet. Chem.* **2010**, *29*, 1–35. Vlček, A., Jr. *Top. Organomet. Chem.* **2010**, *29*, 73–114.

(2) Baker, N. A. C.; McGaughey, N.; Fletcher, N. C.; Chernikov, A. V.; Horton, P. N.; Hursthouse, M. B. *Dalton Trans.* **2009**, 965–972. Fletcher, N. C.; Martin, C.; Abraham, H. J. *New J. Chem.* **2007**, *31*, 1407–1411. Spiccia, L.; Deacon, G. B.; Kepert, C. M. *Coord. Chem. Rev.* **2004**, *248*, 1329–1341.

(3) Koullourou, T.; Natrajan, L. S.; Bhavsar, H.; Pope, S. J. A.; Feng, J. H.; Narvainen, J.; Shaw, R.; Scales, E.; Kauppinen, R.; Kenwright, A. M.; Faulkner, S. *J. Am. Chem. Soc.* **2008**, *130*, 2178–2179.

(4) Kurz, P.; Probst, B.; Spingler, B.; Alberto, R. *Eur. J. Inorg. Chem.* **2006**, 2966–2974.

(5) Kutal, C.; Corbin, A. J.; Ferraudi, G. *Organometallics* **1987**, *6*, 553–557. Kutal, C.; Weber, M. A.; Ferraudi, G.; Geiger, D. *Organometallics* **1985**, *4*, 2161–2166.

(6) Cattaneo, M.; Fagalde, F.; Katz, N. E. *Inorg. Chem.* **2006**, *45*, 6884–6891. Curiel, D.; Beer, P. D. *Chem. Commun.* **2005**, 1909–1911. Higgins, B.; DeGraff, B. A.; Demas, J. N. *Inorg. Chem.* **2005**, *44*, 6662–6669. Louie, M. W.; Liu, H. W.; Lam, M. H. C.; Lau, T. C.; Lo, K. K. W. *Organometallics* **2009**, *28*, 4297–4307. Manimaran, B.; Lai, L. J.; Thanasekaran, P.; Wu, J. Y.; Liao, R. T.; Tseng, T. W.; Liu, Y. H.; Lee, G. H.; Peng, S. M.; Lu, K. L. *Inorg. Chem.* **2006**, *45*, 8070–8077. Sun, S. S.; Lees, A. J. *Chem. Commun.* **2000**, 1687–1688. Tzeng, B. C.; Chen, Y. F.; Wu, C. C.; Hu, C. C.; Chang, Y. T.; Chen, C. K. *New J. Chem.* **2007**, *31*, 202–209.

(7) Fletcher, N. C.; Lagunas, M. C. *Top. Organomet. Chem.* **2009**, *28*, 143–170.

(8) Lo, K. K. W.; Hui, W. K. *Inorg. Chem.* **2005**, *44*, 1992–2002. Lo, K. K. W.; Hui, W. K.; Ng, D. C. M. *J. Am. Chem. Soc.* **2002**, *124*, 9344–9345. Louie, M. W.; Lam, M. H. C.; Lo, K. K. W. *Eur. J. Inorg. Chem.* **2009**, 4265–4273.

(9) Amoroso, A. J.; Arthur, R. J.; Coogan, M. P.; Court, J. B.; Fernandez-Moreira, V.; Hayes, A. J.; Lloyd, D.; Millet, C.; Pope, S. J. A. *New J. Chem.* **2008**, *32*, 1097–1102. Amoroso, A. J.; Coogan, M. P.; Dunne, J. E.; Fernandez-Moreira, V.; Hess, J. B.; Hayes, A. J.; Lloyd, D.; Millet, C.; Pope, S. J. A.; Williams, C. *Chem. Commun.* **2007**, 3066–3068.

(10) Forster, R. J.; Keyes, T. E. *Coord. Chem. Rev.* **2009**, *253*, 1833–1853.

(11) Bertoncello, P.; Kefalas, E. T.; Pikramenou, Z.; Unwin, P. R.; Forster, R. J. *J. Phys. Chem. B* **2006**, *110*, 10063–10069. Jebb, M.; Sudeep, P. K.; Pramod, P.; Thomas, K. G.; Kamat, P. V. *J. Phys. Chem. B* **2007**, *111*, 6839–6844. Terasaki, N.; Akiyama, T.; Yamada, S. *Langmuir* **2002**, *18*, 8666–8671.

(12) Chen, D. T.; De, R.; Mohler, D. L. *Synthesis* **2009**, 211–216.

(13) Jain, P. K.; Huang, X. H.; El-Sayed, I. H.; El-Sayed, M. A. *Acc. Chem. Res.* **2008**, *41*, 1578–1586. Murphy, C. J.; Gole, A. M.; Hunyadi, S. E.; Stone, J. W.; Sisco, P. N.; Alkilany, A.; Kinard, B. E.; Hankins, P. *Chem. Commun.* **2008**, 544–557.

(14) Dieringer, J. A.; McFarland, A. D.; Shah, N. C.; Stuart, D. A.; Whitney, A. V.; Yonzon, C. R.; Young, M. A.; Zhang, X. Y.; Van Duyne, R. P. *Faraday Discuss.* **2006**, *132*, 9–26.

(15) Leyton, P.; Sanchez-Cortes, S.; Garcia-Ramos, J. V.; Domingo, C.; Campos-Vallette, M.; Saitz, C.; Clavijo, R. E. *J. Phys. Chem. B* **2004**, *108*, 17484–17490.

(16) Bell, S. E. J.; Sirimuthu, N. M. S. *Chem. Soc. Rev.* **2008**, *37*, 1012–1024. Drachev, V. P.; Nashine, V. C.; Thoreson, M. D.; Ben-Amotz, D.; Davisson, V. J.; Shalaev, V. M. *Langmuir* **2005**, *21*, 8368–8373. Hidalgo, M.; Montes, R.; Laserna, J. J.; Ruperez, A. *Anal. Chim. Acta* **1996**, *318*, 229–237.

(17) Vlčková, B.; Matejka, P.; Vanoutersterp, J. W. M.; Snoeck, T. L.; Stufkens, D. J. *Inorg. Chem.* **1994**, *33*, 2132–2136.

(18) Ehler, T. T.; Malmberg, N.; Carron, K.; Sullivan, B. P.; Noe, L. J. *J. Phys. Chem. B* **1997**, *101*, 3174–3180.

(19) Hallett, A. J.; Christian, P.; Jones, J. E.; Pope, S. J. A. *Chem. Commun.* **2009**, 4278–4280.

(20) Pelleteret, D.; Fletcher, N. C.; Doherty, A. P. *Inorg. Chem.* **2007**, *46*, 4386–4388.

(21) Pelleteret, D.; Fletcher, N. C. *Eur. J. Inorg. Chem.* **2008**, 3597–3065.

(22) Wolcan, E.; Torchia, G.; Tocho, J.; Piro, O. E.; Juliarena, P.; Ruiz, G.; Feliz, M. R. *J. Chem. Soc., Dalton Trans.* **2002**, 2194–2202.

(23) Hevia, E.; Perez, J.; Riera, V.; Miguel, D.; Kassel, S.; Rheingold, A. L. *Inorg. Chem.* **2002**, *41*, 4673–4679. Klein, A.; Vogler, C.; Kaim, W. *Organometallics* **1996**, *15*, 236–244.

(24) Fletcher, N. C.; Brown, R. T.; Doherty, A. P. *Inorg. Chem.* **2006**, *45*, 6132–6134. Telfer, S. G.; Bernardinelli, G.; Williams, A. F. *Dalton Trans.* **2003**, 435–440.

(25) Panetta, C. A.; Kumpaty, H. J.; Heimer, N. E.; Leavy, M. C.; Hussey, C. L. *J. Org. Chem.* **1999**, *64*, 1015–1021.

(26) Leopold, N.; Haberkorn, M.; Laurell, T.; Nilsson, J.; Baena, J. R.; Frank, J.; Lendl, B. *Anal. Chem.* **2003**, *75*, 2166–2171.

(27) *SERS Processing Software*, 8.0 ed.; Thermo Fisher Scientific Inc.: St. Louis, MO, 2007.

(28) Frisch, M. J.; Trucks, G. W.; Schlegel, H. B.; Scuseria, G. E.; Robb, M. A.; M. A.; Cheeseman, J. R.; Montgomery, J. A., Jr.; Vreven, T.; Kudin, K. N.; Burant, J. C.; Millam, J. M.; Iyengar, S. S.; Tomasi, J.; Barone, V.; Mennucci, B.; Cossi, M.; Scalmani, G.; Rega, N.; Petersson, G. A.; Nakatsuji, H.; Hada, M.; Ehara, M.; Toyota, K.; Fukuda, R.; Hasegawa, J.; Ishida, M.; Nakajima, T.; Honda, Y.; Kitao, O.; Nakai, H.; Klene, M.; Li, X.; Knox, J. E.; Hratchian, H. P.; Cross, J. B.; Adamo, C.; Jaramillo, J.; Gomperts, R.; Stratmann, R. E.; Yazyev, O.; Austin, A. J.; Cammi, R.; Pomelli, C.; Ochterski, J. W.; Ayala, P. Y.; Morokuma, K.; Voth, G. A.; Salvador, P.; Dannenberg, J. J.; Zakrzewski, V. G.; Dapprich, S.; Daniels, A. D.; Strain, M. C.; Farkas, O.; Malick, D. K.; Rabuck, A. D.; Raghavachari, K.; Foresman, J. B.; Ortiz, J. V.; Cui, Q.; Baboul, A. G.; Clifford, S.; Cioslowski, J.; Stefanov, B. B.; Liu, G.; Liashenko, A.; Piskorz, P.; Komaromi, I.; Martin, R. L.; Fox, D. J.; Keith, T.; Al-Laham, M. A.; Peng, C. Y.; Nanayakkara, A.; Wong, M. W.; Gonzalez, C.; Pople, J. A.; Gaussian, I. *Gaussian03*; Gaussian, Inc.: Pittsburgh, PA, 2003.

(29) Becke, A. D. *J. Chem. Phys.* **1993**, *98*, 5648–5652.Lee, C. T.; Yang, W. T.; Parr, R. G. *Phys. Rev. B.* 1988, *37*, 785−789.

(30) Hay, P. J.; Wadt, W. R. *J. Chem. Phys.* **1985**, *82*, 299–310.

(31) Sendroiu, I. E.; Schiffrin, D. J.; Abad, J. M. *J. Phys. Chem. C* **2008**, *112*, 10100–10107. Rooth, M.; Shaw, A. M. *J. Phys. Chem. C* **2007**, *111*, 15363–15369.

(32) Sacksteder, L.; Zipp, A. P.; Brown, E. A.; Streich, J.; Demas, J. N.; DeGraff, B. A. *Inorg. Chem.* **1990**, *29*, 4335–4340. Wrighton, M.; Morse, D. L. *J. Am. Chem. Soc.* **1974**, *98*, 998–1003. Yam, V. W. W.; Qi, G. Z.; Cheung, K. K. *J. Chem. Soc., Dalton Trans.* **1998**, 1819–1823.

(33) Vlček, A., Jr.; Zalis, S. *Coord. Chem. Rev.* **2007**, *251*, 258–287.

(34) Dattelbaum, D. M.; Martin, R. L.; Schoonover, J. R.; Meyer, T. J. *J. Phys. Chem. A* **2004**, *108*, 3518–3526.

(35) Stoyanov, S. R.; Villegas, J. M.; Cruz, A. J.; Lockyear, L. L.; Reibenspies, J. H.; Rillema, D. P. *J. Chem. Theory Comput.* **2005**, *1*, 95–106.

(36) Howell, S. L.; Scott, S. M.; Flood, A. H.; Gordon, K. C. *J. Phys. Chem. A* **2005**, *109*, 3745–3753. Machura, B.; Kruszynski, R. *Polyhedron* **2007**, *26*, 3336–3342.

(37) Machura, B.; Kruszynski, R.; Kusz, J. *Polyhedron* **2007**, *26*, 1590–1596.

(38) Kudelski, A. *Vib. Spectrosc.* **2005**, *39*, 200–213.

(39) Bensebaa, F.; Zhou, Y.; Brolo, A. G.; Irish, D. E.; Deslandes, Y.; Kruus, E.; Ellis, T. H. *Spectrochim. Acta A* **1999**, *55*, 1229–1236. Shen, A. J.; Pemberton, J. E. *J. Electroanal. Chem.* **1999**, *479*, 21–31.

(40) Kim, M.; Itoh, K. *J. Electroanal. Chem.* **1985**, *188*, 137–151.

(41) Kim, M.; Itoh, K. *Organometallics* **1987**, *91*, 126–131. Srnova, I.; Vlckova, B.; Nemec, I.; Slouf, M.; Stepanek, J. *J. Mol. Struct.* **1998**, *482*−*483*, 213–216.

(42) Clark, I. P.; George, M. W.; Johnson, F. P. A.; Turner, J. J. *Chem. Commun.* **1996**, 1587–1588. George, M. W.; Johnson, F. P. A.; Westwell, J. R.; Hodges, P. M.; Turner, J. J. *J. Chem. Soc., Dalton Trans.* **1993**, 2977–2979. Tan, H.; Wong, L. K.; Lai, M. Y.; Kiruba, G. S. M.; Leong, W. K.; Wong, M. W.; Fan, W. Y. *J. Phys. Chem. B* **2005**, *109*, 19657–19663.

(43) Bredenbeck, J.; Helbing, J.; Hamm, P. *J. Am. Chem. Soc.* **2004**, *126*, 990–991.

(44) Schoonover, J. R.; Strouse, G. F.; Dyer, R. B.; Bates, W. D.; Chen, P. Y.; Meyer, T. J. *Inorg. Chem.* **1996**, *35*, 273–274.

(45) Omberg, K. M.; Schoonover, J. R.; Meyer, T. J. *J. Phys. Chem. A* **1997**, *101*, 9531–9536. Schoonover, J. R.; Strouse, G. F. *Chem. Rev.* **1998**, *98*, 1335–1355.